INDONESIAN JOURNAL ON GEOSCIENCE
Geological Agency
Ministry of Energy and Mineral Resources

Journal homepage: http://ijog.geologi.esdm.go.id
ISSN 2355-9314, e-ISSN 2355-9306

ASTER Mineral Classification for Regolith Mapping in Tick Hill Mount Isa, Northwest Queensland

Fitriani Agustin

Geological Survey Institute, Geological Agency Bandung, Indonesia
Jln. Diponegoro No. 57 Bandung

Corresponding author: afitchan@gmail.com
Manuscript received: January 21, 2016; revised: September 5, 2016;
approved: June 19, 2017; available online: July 7, 2017

Abstract - This paper analyzed the mineral maps of AlOH bearing minerals and iron oxide using ASTER imagery in Tick Hill, Mount Isa, northwestern part of Queensland, as a guide for mapping the regolith unit within the area. Tick Hill is part of the Proterozoic Eastern and Western Fold Belt Province (Mount Isa Inlier Complex) covered by Mesozoic and Paleozoic lithologies and dominated by medium to coarse hornblende-biotite granite and gneiss; both of which intruded during 1760 - 1720 Ma. Highly weathered landforms cover the whole area. The Mesozoic sediments have experienced deep weathering, and currently present in the form of mesas. The weathering profiles are dominated by kaolinite, smectite, and pedogenic carbonates with some secondary silicification. Part of the landform is covered by colluvium varying in thickness from less than 1 m up to 12 m in certain places. Digital image processing has been done to ASTER imagery, *i.e*: calibrating, mosaicing, and band ratioing and false colour RGB. Within these methods, iron oxide, kaolinite, AlOH, and MgOH group mineral maps have successfully been created through the ASTER imagery. Later, these mineral maps were applied to interpret the surface regolith mapping unit. In addition, field samples have been taken in regolith covered areas to validate the ASTER mineral information.

Keywords: ASTER, mineral mapping, regolith mapping, Tick Hill

How to cite this article:
Agustin, F., 2017. ASTER Mineral Classification for Regolith Mapping in Tick Hill Mount Isa, Northwest Queensland. *Indonesian Journal on Geoscience*, 4 (2), p.97-109. DOI: 10.17014/ijog.4.2.97-109

Introduction

Cudahy *et al*. (2008) defined mineral mapping as a particular interaction of geological materials with electromagnetic radiation anywhere across the wavelength range between 400 nm to 14,000 nm. Mineral mapping relies on spectral characteristics of minerals which are in turn dependant on mineral composition (Hunt, 1977; Clark, 1999).

The advent of multispectral sensors has improved the rapid surface mapping of minerals and earth materials. ASTER imagery, as one of the multispectral sensors, can recognize mineral groups in the VNIR - SWIR range, and the data after processing allow potential mapping of minerals. The ASTER sensor has been employed to make mineral maps in Australia (Hewson *et al*., 2005; Oliver and van der Wielen, 2006) and other parts of the world (Rowan and Mars, 2003; Mars and Rowan, 2006). These sensors have allowed the mapping of spectrally sensitive minerals in the VNIR and SWIR and also in thermal range, namely AlOH, MgOH, FeOH bearing minerals,

iron oxides, and carbonates. Many of the minerals identified and mapped are important, as their presence and distribution are linked to hydrothermal alteration, such as AlOH bearing phyllosilicates (muscovite, illite, kaolinite), MgOH bearing phyllosilicates (chlorite) and carbonates, and also to regolith materials such as kaolinite, iron oxides, and carbonates. There are several processing methods available to make mineral maps and the validity and effectiveness of each need to be established for specific surface materials. For example for the multispectral ASTER sensor, band ratio, or relative band depth have been employed to distinguish specific minerals or mineral assemblages (Hewson *et al*., 2006; Mars and Rowan, 2006).

In Australia, where regolith covers much of the continent, mapping regolith material distribution is vital to many applied disciplines, such as selection of appropriate sample media for geochemical exploration (Anand and Paine, 2002; Butt, 2005). Therefore, any technique which rapidly and effectively maps the surface minerals can aid the interpretation of an insight into geology and regolith evolution of an area as well as optimize mineral exploration. Although remote sensing has been used to map and identify regolith (Tapley and Gozzard, 1992), the full potential of employing individual minerals and mineral assemblage maps to map the regolith and subsequently interpret the regolith processes and landform evolution of selected areas has not been explored.

This paper aims to map surface mineral: iron oxide and AlOH bearing minerals, using ASTER VNIR and SWIR ranges. The studied area is part of The Smart Exploration Project programme announced by CSIRO Exploration and Mining and Geological Survey of Queensland, located within 21° 14’ 1’’ - 21° 43’ 24.24’’ South and 139° 47’ 47.04’’ - 140° 1’ 19.20’’ East, Tick Hill, northern-central part of Queensland (Figure 1).

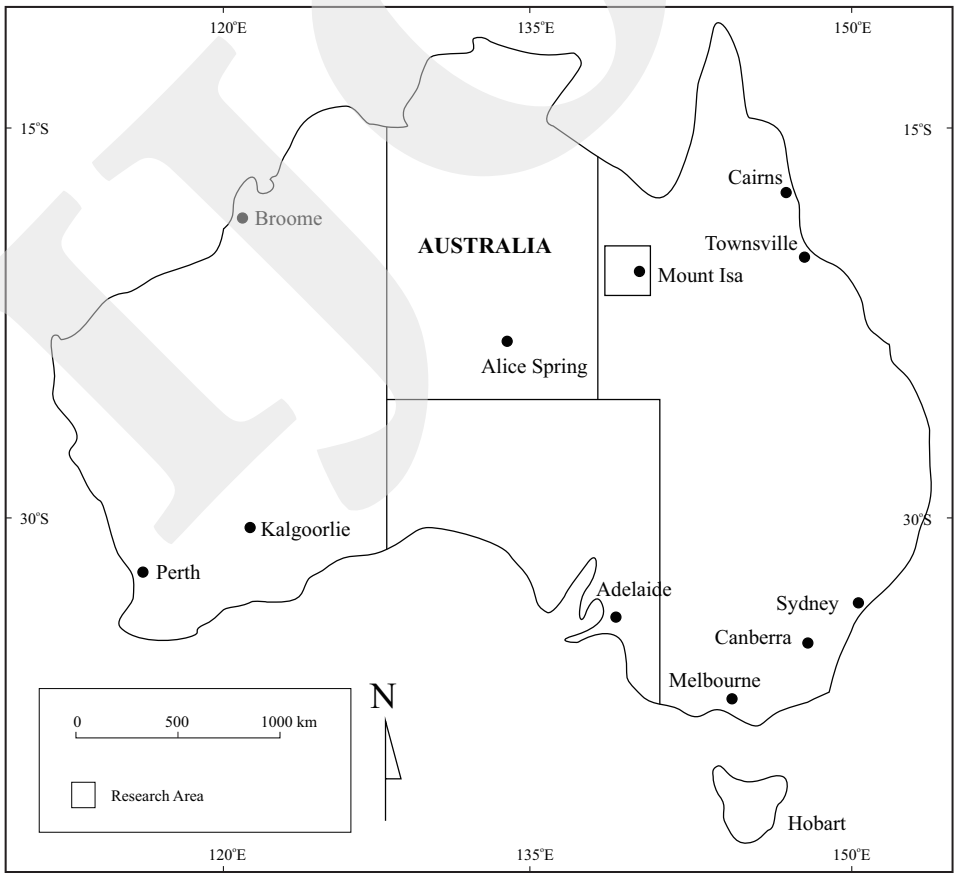

Figure 1. Locality map of the studied area.

Regional Geology and Regolith Setting

The basement of the area comprises Proterozoic rocks that outcrop within northern-western part of Queensland represented by the Mount Isa Province. The province is divided into three subprovinces: the Kalkadoon-Leichhardt, the Eastern, and the Western Fold Belt (Geological Survey of Queensland, 2011). The studied area is in Tick Hill region which is located in the Eastern and Western Fold Belt Province. Those protoliths mainly consist of marine sediments and some products of volcanism. Rocks in this area have strongly been affected by regional metasomatism in high degree. The rocks of this basements were then intruded by granite plutons and mafic rocks as dykes, sills, and hypabissal felsic intrusions. The intrusions of the basement occured at various episodes: the Sybella granites in the Western Fold Belt Province (around 1670 Ma), the Kalkadoon and Ewen granites in the Kalkadoon-Leichhardt Domain (around 1870 - 1850 Ma), the Wonga granites in the Mary Kathleen Domain (1750 - 1725 Ma), and the Williams granites (around 1500 Ma) in the Eastern Fold Belt (Figure 2). The historical deformation of Mount Isa Complex occured in

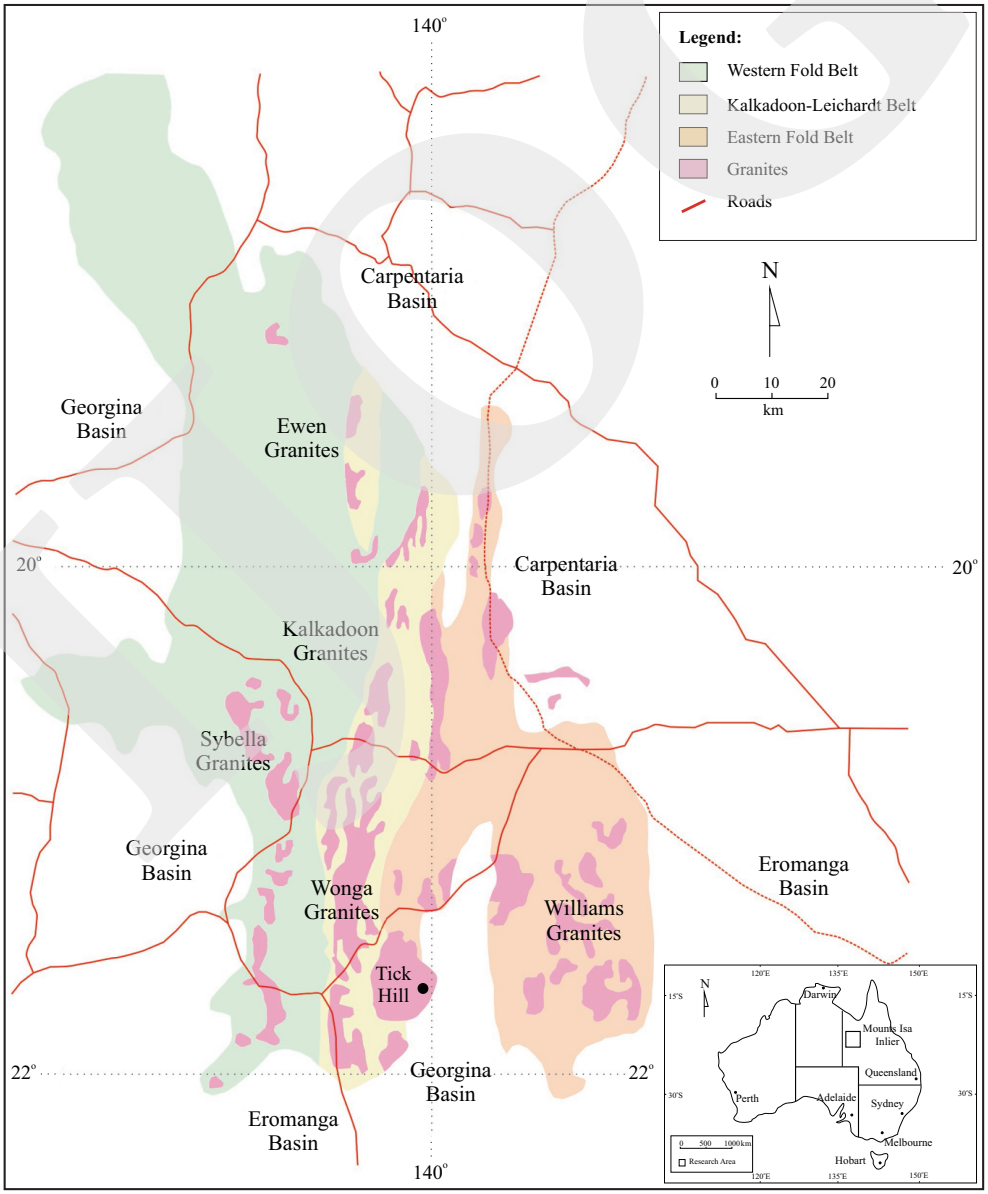

Figure 2. Simplified regional geology setting of Mount Isa Complex (Geological Survey of Queensland, 2011).

different periods; the basement were strongly folded and in some parts melted. Thrusting and folding occured around 1620 Ma where compression trended east-west. It formed the north-south fault trending in Mount Isa Province (Eriksson *et al*., 1991; Blake, 1987). The following extention periods were represented by numerous granites and mafic rock intrusions. The main faults in this province are dominantly strike-slip which were active during the Proterozoic and some were active during Phanerozoic. In terms of economic geology, these rocks are potential for precious mineral deposits mainly including base metals (Pb, Zn, Ag, Cu, and Au).

Anand *et al.* (2002a) conducted a regolith research in some parts of Mount Isa region and they concluded that regolith distribution and genesis in Mount Isa region was complex due to multiple weathering, erosion, and depositional episodes during the Mesozoic and Cenozoic Era.

Anand *et al.* (2002) have divided regolith-landforms in Mount Isa region into three basic provinces, namely hill belts, undulating terrain, and plains, each being characterized by its degree of weathering, erosion, and depositions. Highly weathered landforms covered the whole area. The Mesozoic sediments have experienced deep weathering and currently present in the form of mesas. The weathering profiles are dominated by kaolinite, smectite, and pedogenic carbonates with some secondary silicification. Part of the landform is covered by colluvium which varied in thickness from less than 1 m up to 12 m in certain places. The deep weathering profiles observed in the region are similar to those of an ideal lateritic profile described by Nahon and Tardy (1992), Taylor and Eggleton (2001), and Anand and Paine (2002) where the uppermost soil is underlain by duricrust, then by mottled zone followed by saprolite and then saprock. Anand *et al.* (2002) found that the weathering profile in Proterozoic and Mesozoic rocks was controlled by bedrock composition and paleotopography. The profiles in the Mount Isa region from the top to the base are composed of lateritic nodules and pisoliths, pockets of duricrust, indurated ferruginous saprolite, a clay zone, saprolite (silicified in part), saprock, and bedrock (Figure 3).

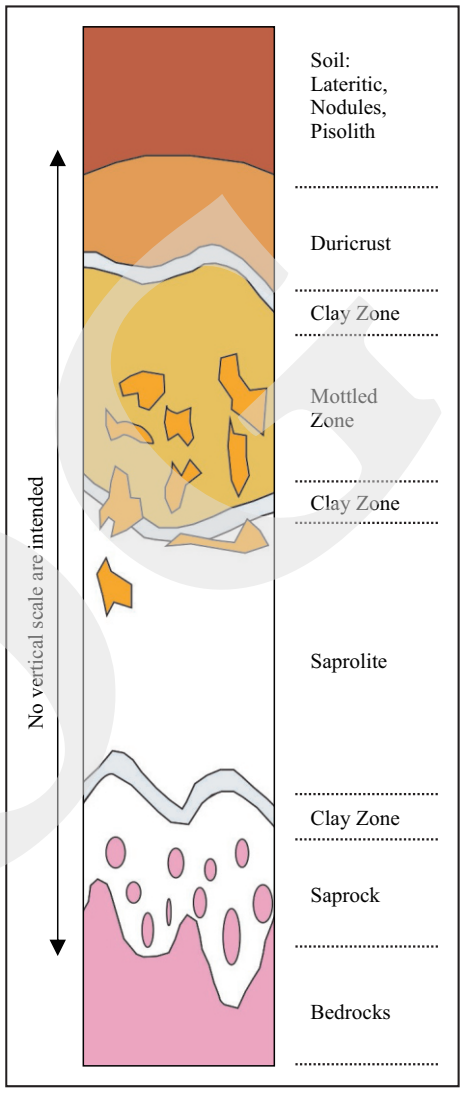

Figure 3. Simplified regional regolith profile of Mount Isa and surrounding areas (modified from Taylor and Eggleton, 2001).

Materials and Methods

ASTER dataset

The Advance Spaceborne Thermal Emission and Reflection Radiometer (ASTER) is a joint science project between METI Japan and NASA launched in December 1999 as a multispectral sensor onboard the TERRA, NASA's Earth Observed system satellite. It records reflected and emitted solar radiation into fourteen wavelength

ranges (spectral bands). Three 15 m bands are recorded in VNIR). The shortwave infrared (SWIR) reflected wavelength is recorded in 6 bands with a spatial resolution of 30 m and the thermal infrared (TIR) radiation is recorded in 5 bands with a spatial resolution of 90 m. Each acquired scene covers an area of 60 x 60 km width (Iwasaki and Fujisada, 2005) (Table 1).

ASTER Image Processing and Interpretation

The pre-processing of 14 single bands of ASTER Level 1B has been done; atmospheric correction, radiometric and geometric calibration, cross-talked correction, and resampling and mosaicing images. For image interpretation method, RGB combination and Band Ratio (BR) were applied to map the surface minerals.

The ASTER dataset were in radiance at sensor (level 1B) which have already been corrected both radiometrically and geometrically. Then, those are converted from the radiance to the reflectance images. The resampling process was created for VNIR and SWIR images into 30 m resolution using ENVI software through Layer Stacking Process (ENVI online tutorial). The two ASTER scenes were mosaiced to create a seamless image using Map Based Mosaic in ENVI.

The RGB model is based on assigning a single band or band ratios to primary colours (red, green, blue) to enhance specific spectral characteristics for easy visual interpretation. Several factors that should be considered before trying to match RGB combination are: screening and selecting the appropriate bands which included the atmospheric effects, knowledge of ground material spectra and the object of interests such as vegetation, rock outcrops, morphology, plain terrain, man-made buildings, and the method for trial experiment (Gupta, 2003).

The Band Ratio method is a simple method dividing the DN (digital number) of each pixel in one band by the DN for equivalent pixels in another band. The bands chosen should have a contrast in their absorption for the specific of minerals or surface material under consideration. The process will result in reducing topographic features of the image (Drury, 2001). The band ratio has successfully been used to map lithological variations based on mineral composition (van Ruitenbeek *et al*. 2006).

The band ratio of (b4/b3), (b7/b5), ((b5+b7/b6), and (b6+b8)/b7) were applied to map the iron oxide, kaolinite, AlOH, and MgOH bearing minerals respectively. The 2 % linear stretch

Table 1. ASTER Bands Wavelength (Iwasaki and Fujisada, 2005)

Band number	Wavelength (micrometer)	Wavelength name	Resolution (m)
Band 1	0.25 to 0.60	visible green	15
Band 2	0.63 to 0.69	visible red	15
Band 3	0.76 to 0.86	near infra red	15
Band 4	1.60 to 1.70	shortwave infra red	30
Band 5	2.145 to 2.185	shortwave infra red	30
Band 6	2.185 to 2.285	shortwave infra red	30
Band 7	2.235 to 2.285	shortwave infra red	30
Band 8	2.295 to 2.365	shortwave infra red	30
Band 9	2.360 to 2.430	shortwave infra red	30
Band 10	8.125 to 8.475	thermal infra red	90
Band 11	8.475 to 8.825	thermal infra red	90
Band 12	8.925 to 9.275	thermal infra red	90
Band 13	10.25 to 10.95	thermal infra red	90
Band 14	10.95 to 11.65	thermal infra red	90

was applied on those histogram, then performed in rainbow colour scale. The detail steps of ASTER mineral mapping processing are explained in Figure 4.

Spectral Laboratory Measurement

Field sample spectra measurements were at first conducted by CSIRO team for Queensland mineral project using Analytical Spectral Devices (ASD) fieldspec Pro I which has the spectral range of 350 - 2.500 nm. The selected group was measured in duplicate by the author. The ASD collected spectra were viewed and analyzed via the The Spectral Geologist (TSG) (http://www.thespectralgeologist.com/). Field samples were taken from sixteen field sites located within the Tick Hill region (Figure 2). Seventy-eight reflectance spectra were acquired from samples collected from sixteen locations. For most locations, several samples were collected and analyzed via the ASD in the field, and again in the laboratory. Many locations had more than one variety of samples depending on the sample type and degree of weathering. The types of samples fell into three categories: fresh rocks, weathered rocks (saprock and saprolite), and soil samples. Most of the field samples were located in the regolith covered areas (weathered rocks and surficial deposits). The ASD acquired spectra were used to validate the ASTER mineral maps. The ASD spectra were at first resampled to the sensor band widths, and then the same Ratio Band Depth (RBD) was used to make individual mineral maps of which ASTER was employed on the resampled ASD spectra. The measured values from ASD RBD were then plotted against band depth values estimated from spectra for pixels representing corresponding field sample.

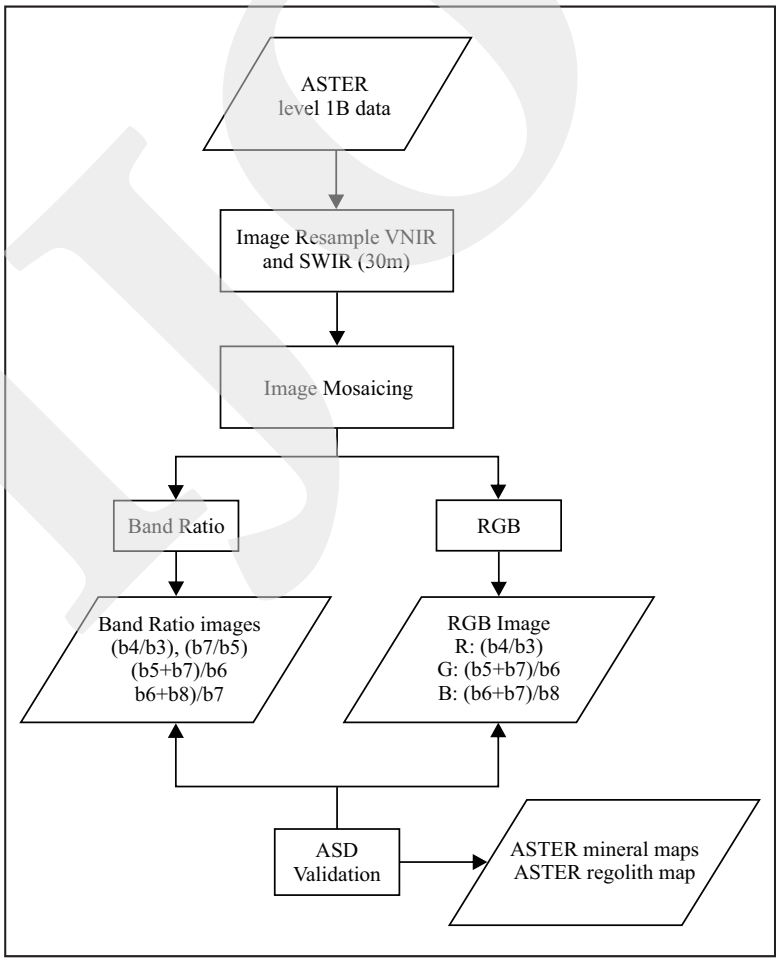

Figure 4. ASTER image processing flow chart.

Result and Discussion

Mineral Mapping

Through ASTER images, there are four main minerals related to the weathering process can be identified; iron oxide, kaolinite, AlOH (white mica, Al-Smectite), and MgOH group (Figure 5). In addition, vegetation index was also mapped through the Normalized Difference Vegetation Index method to mask all the mineral maps produced.

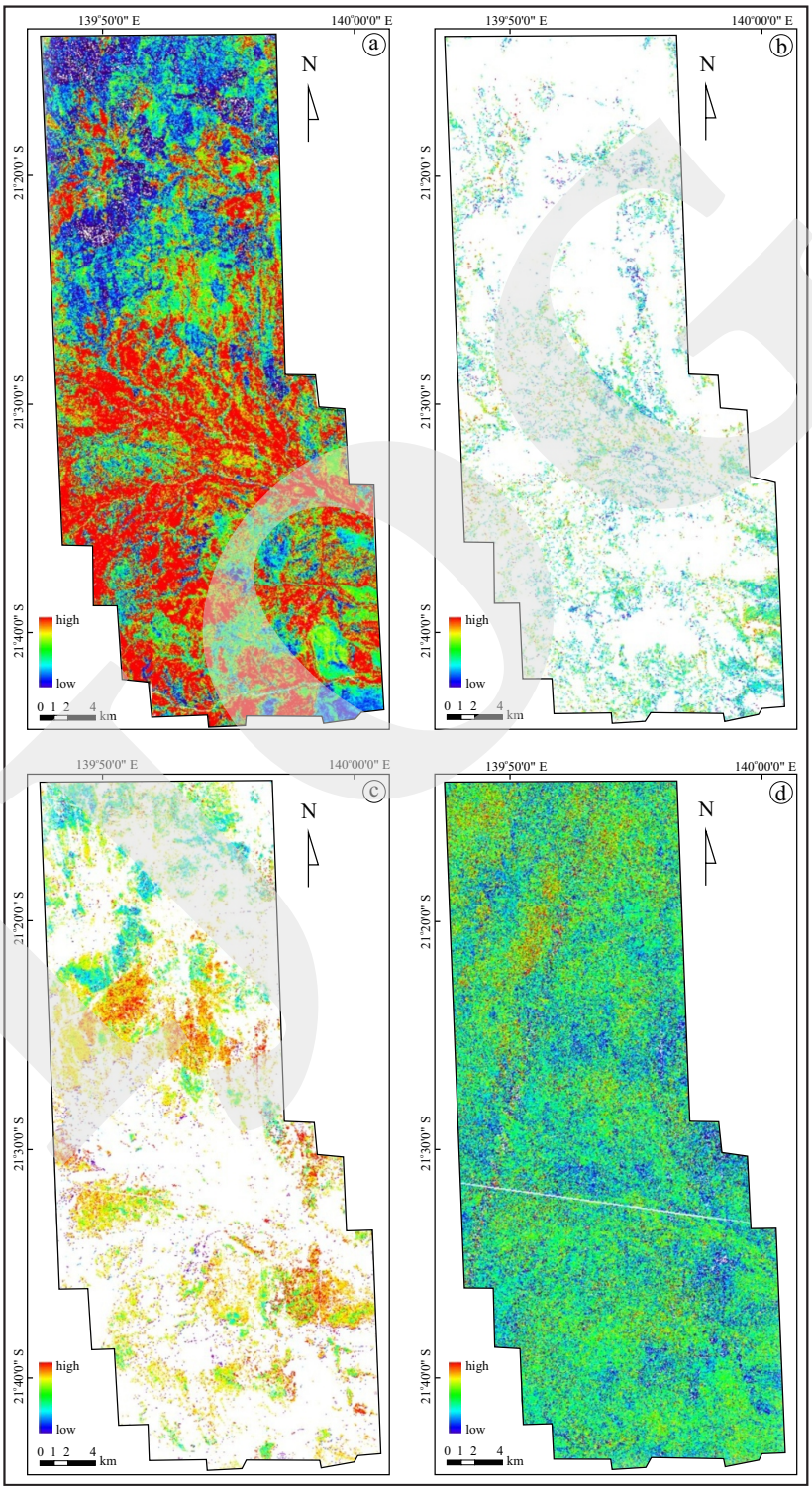

Figure 5. ASTER mineral map products; iron oxide (a), kaolinite (b), AlOH (c), and MgOH group (d).

Iron-Oxide mapping using ASTER Image

The iron oxide (total hematite and goethite) surface map is constructed using the band ratio (4/3) as this band wavelength ratio highlights ferric iron (hematite and goethite) (Rowan and Mars, 2003; Hewson *et al*., 2005; Gozzard, 2006). The high abundance of iron oxide appears associated with Recent alluvial and colluvial deposits that dominate the middle of Block G Tick Hill area (Figure 5a). However, the iron oxide distribution appears to correlate with vegetation distribution, namely along the drainages. This could be due to the absorption features of iron oxides as seen in the broad bands of ASTER, which are close to the vegetation absorption peaks (Lewis, 2002).

Kaolinite mapping using ASTER Image

The kaolinite map was produced from ASTER and took into account a map of kaolin group minerals such as halloysite, dickite, and kaolinite. Extracting spectra pattern of kaolinite in ASTER is done by resampling USGS library spectra of kaolinite to fit the ASTER band positions. Band ratio b7/b5 was used, where band 7 (2.23 μm - 2.28μm) has the maximum reflectance of kaolinite (2,200 nm) and band 5 (2.145 μm - 2.185 μm) has relatively minimum absorption at 2,160 nm. These two bands are suitable for ASTER data to obtain kaolin group abundance (Rowan and Mars, 2003; Hewson *et al*., 2005). As other AlOH bearing minerals might interfere with the kaolin group at 2,200 nm, the RBD for AlOH absorption (b5+b7)/b6 and band ratio index b5/b6 for white mica composition were created to mask kaolinite.

It is assumed that all AlOH absorption feature centred at 2,200 nm such as Al-mica and possibly illite and smectite have been removed and only kaolin group minerals are highlighted. Figure 5b shows the kaolin group abundance derived from band ratio 7/5, after masking out the AlOH at 2,200 nm and Al-mica on band ratio 5/6. The false colour composite of red indicates high abundance of kaolin group, and blue colour suggests low abundance of kaolinite group. The black colour indicates the absence of kaolinite. Comparison of the spatial distribution of kaolin minerals with mapped lithology suggests that kaolin is predominantly present on the surface as mapped for recent deposits and also for some Precambrian rocks. The distribution of kaolin is linked to regolith material distribution, and this is not clearly expressed in the geology map.

AlOH and MgOH mineral group mapping using ASTER Image

The term white mica includes the group sericite-muscovite-illite. To identify white micas and Al-smectite as individual minerals with ASTER is difficult because of the broad bandwidth of SWIR bands of the ASTER sensor (approximately 40 nm bandwidth) (Fujisada, 1994). Therefore, only Al-OH mineral group as a whole can be distinguished rather than individual AlOH bearing minerals. Several researchers have employed the band ratio (5+7)/6 to discriminate AlOH minerals such as sericite-muscovite-illite-smectite from other non AlOH bearing minerals (Rowan and Mars, 2003; Hewson *et al*., 2005; Rowan *et al*., 2005; Rowan *et al*., 2006). It highlights the AlOH bearing minerals occurring in the 2.14 μm - 2.28 μm and have been used to produce white mica-Al-smectite maps from the ASTER data. As shown in Figure 5c, the distribution of white mica and Al-smectite minerals as mapped via ASTER data, shows a higher occurrence in Precambrian rocks which are located in northern and the southwestern part of the mapped area. There appears to be variation in the abundance of AlOH group minerals within the Precambrian rocks, and this could be due to variation in white mica in the rocks themself, or due to weathering of the rocks.

The ASTER band ratio of (6+8)/7 was used to produce carbonate and MgOH mineral map of the area. It was employed to highlight carbonates, chlorite, and epidote (Rowan and Mars, 2003; Hewson *et al*., 2004). The image in Figure 5d shows that carbonates and MgOH group mineral are concentrated in the northern part of Tick Hill region which is occupied by Precambrian rocks composed mainly of meta-volcanic, foli-

ated granite, pegmatite, and gneiss. The MgOH minerals mapped seem to be present over fresh to weathered Precambrian rocks and are likely due to either primary mineral (amphiboles) or alteration minerals, mainly chlorites and carbonates. It is important to note that the broad band nature of ASTER sensor precludes identifying individual CO3 and Mg-OH bearing minerals from their main absorption features that subtly vary in wavelength in the 2,300 nnm range. Therefore, pure carbonate and MgOH spectra are difficult to separate in the image. Furthermore, the carbonate signal is affected by residual crosstalk errors which are most noticeable in low albedo areas.

Mineral Mapping Validation

Figure 6 represents the correlation between ASTER mineral maps produced against the resampled ASD field spectra measurements through ASTER band width. The ASTER iron oxides map shows moderate result at R2= 0.519. This result confirms that ASTER band ratios are not very effective in mapping iron oxides and one reason could be the influence of vegetation within the bands chosen. However, the high correlation of R2= 0.96 is shown in kaolinite map validation. It means that that ASTER kaolinite band ratio is effective in mapping kaolin group of minerals. Validation of AlOH bearing minerals (besides kaolinite) - sericite-muscovite-illite-smectite- was conducted for ASTER band ratio (5+7)/6 against laboratory spectra (ASD) for specific field samples showed a good correlation (R2=0.8877 for illite-muscovite). While the correlation coefficient of R2 = 0.9013 has been resulted from MgOH bearing mineral map. It suggests that the method is effective in mapping carbonates and MgOH bearing minerals together.

ASTER Regolith Mapping

To map regolith on a regional scale, a simple RGB (Red-Green-Blue) combination method is used to reveal different spectral classes of surface materials. The three mineral maps created from ASTER (Figure 5) are used to delineate regolith material units.

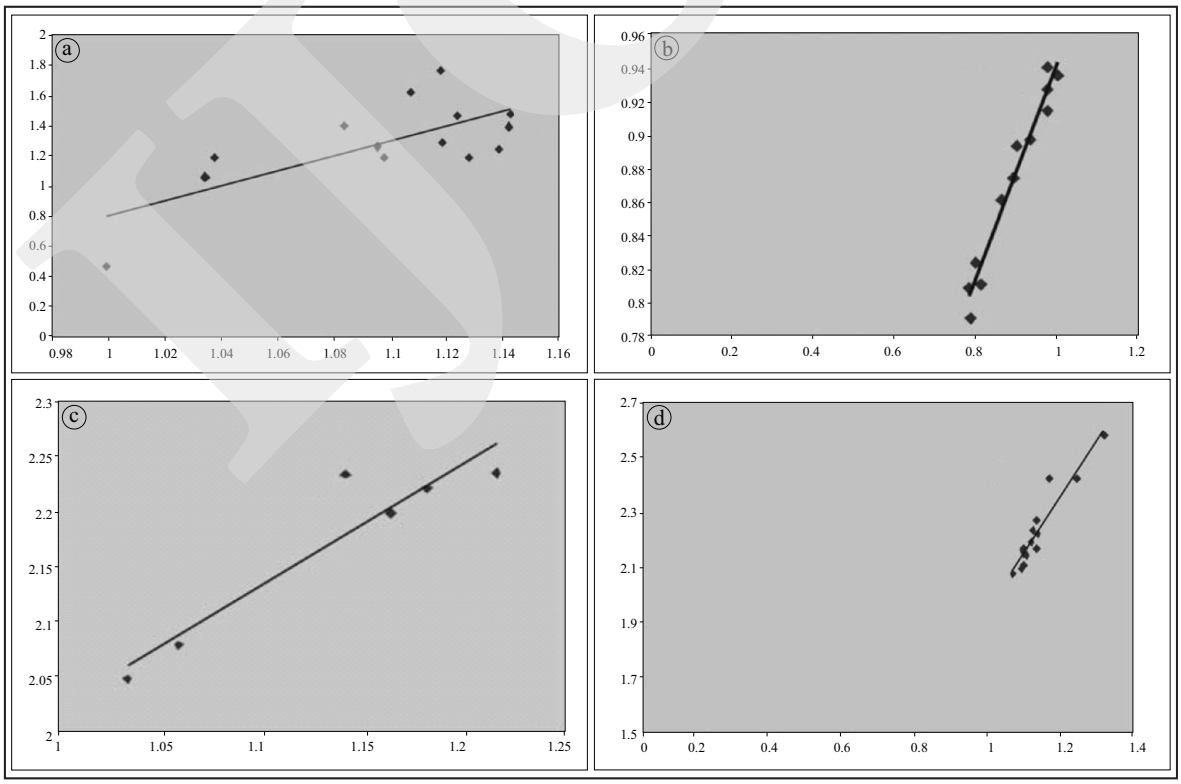

Figure 6. Validation scatter plot diagrams of ASTER iron oxides(a), kaolinite (b), AlOH (c), and MgOH group (d) against calculated ASD spectral of field samples resampled to ASTER band widths.

The RGB combination of R (band 4/band 3), G (band 5+band 7/band 6), and B (band 6+band 7/band 8) of Block G Tick Hill differentiate well between highly weathered materials (red-yellow) and variably weathered bedrock exposures (purple-greenish-bluish) (Figure 7).

The interpretation of ASTER RGB image (Figure 7) shows that blue - purple colours are interpreted as materials rich in MgOH bearing minerals. Green to yellowish colours were interpreted as materials composed of AlOH bearing minerals and the red colours as materials rich in

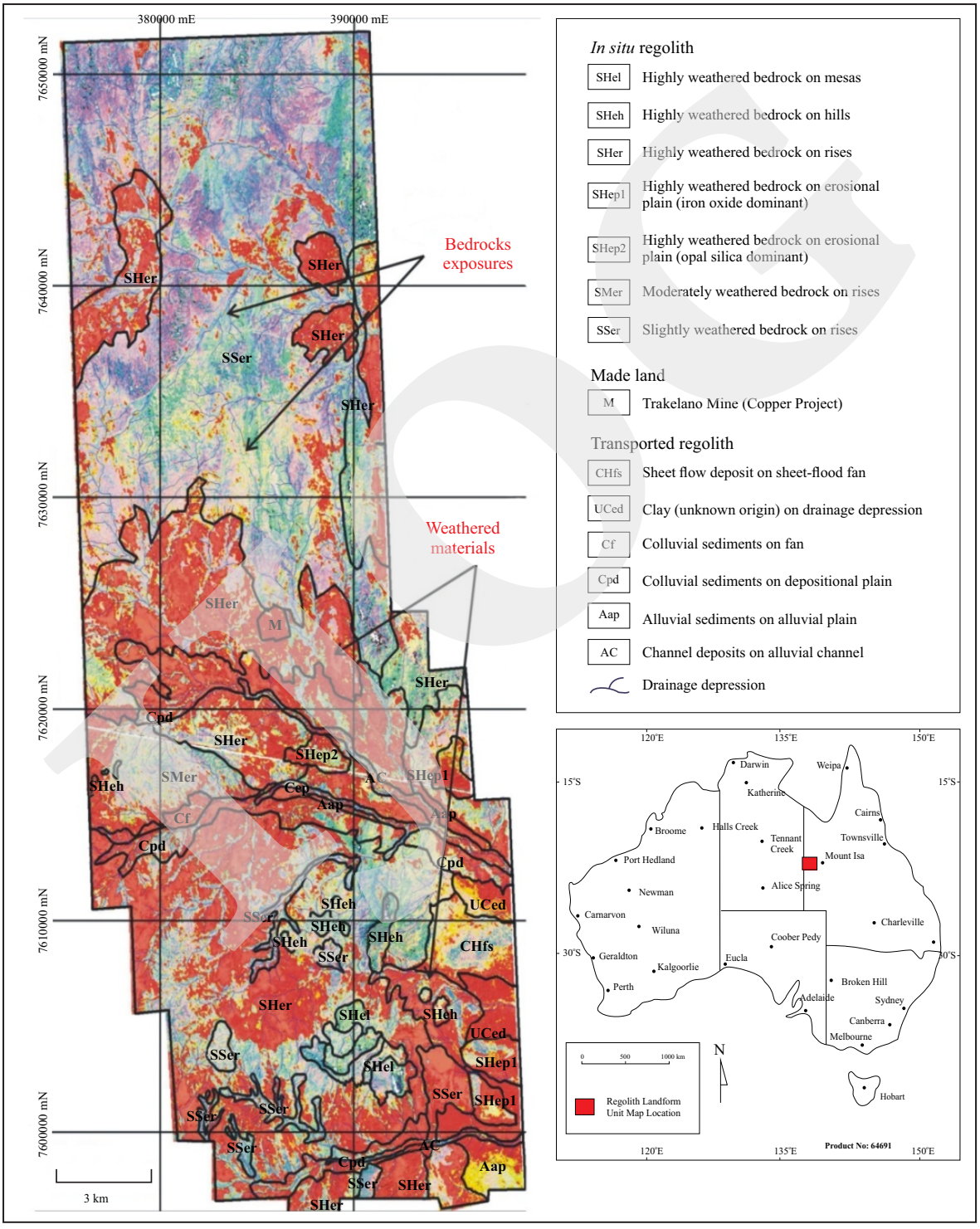

Figure 7. ASTER surface regolith mapping in Tick Hill, Mount Isa, northern part of Queensland.

iron oxide. Moreover, bedrock related signatures of high MgOH content from primary MgOH bearing minerals such as chlorites, amphiboles, and serpentines and AlOH in micas are dominant to the north. They are mainly within the topographically higher landforms such as hills and rises and are represented by the purple - bluish-greenish colours. The highly weathered bedrocks appear as red to pale yellows and the less weathered bedrocks are expressed in light green to magenta and purple, and are a reflection of high AlOH (kaolinite) and iron oxides.

The ASTER RGB image appears effectively in highlighting variation in weathering degree of the bedrock as seen from variation in the colour indicative of bedrock. Therefore, the results imply that the northern part of the area is dominated by slightly weathered bedrock, while the southern part is dominated by a combination of slightly weathered bedrock and highly weathered bedrock. Transported regolith in the form of colluvium and alluvium also mantles the southern-central part of the studied area. The colluvium occurs as highly weathered regolith materials exposed in the low land areas which correspond to red images rich in iron oxide and yellow to greenish images content mix between iron oxides and AlOH.

Surface regolith map were created based on ASTER RGB image interpretation according to colour variation related to minerals. There are two general regolith landform units categorized: *in situ* regolith and transported regolith. Also, the man-made land is enclosed for the different object on the surface. The *in situ* regolith consists of Highly weathered bedrock underlying mesas and adjoining slopes (SHel), Highly weathered material on hills (SHeh), Highly weathered material on erosional rises (SHer), Highly weathered bedrocks on erosional plain with iron oxide dominant (SHep1), Highly weathered bedrocks on erosional plain where opal silica dominant (SHep2), Moderately weathered bedrock on erosional rise (SMer), Slightly weathered bedrock on erosional rise (SSer), and Made land (M). The transported regolith comprises Sheet flow deposit on sheet-flood fan (CHfs), Clay of Unknown Origin on drainage depression (UCed), Colluvial sediments on fan (Cf), Colluvial sediments in depositional plain (Cpd), Alluvial sediment on alluvial Plain (Aap), and Channel Deposit (ACa) (Figure 7).

Conclusions

ASTER mineral maps are able to map mineral groups such as AlOH and MgOH bearing minerals, but not so effective to map iron oxide minerals. However, due to lack of resolution, ASTER performed less accurate mineral map delineation. In terms of regolith mapping, the regolith mineral map can guide us for performing field observation to validate the regolith material units identified through ASTER RGB mineral map interpretation. Further research on high spectral resolution image, *i.e.* Hyperspectral imagery, is recommended especially to find suitable methods to differentiate the AlOH bearing minerals which have slightly different absorption within the 2,200 nm wavelength range for different clay minerals.

Acknowledgements

This research is part of joint collaboration between CSIRO Exploration and Mining and Queensland Geological Survey. The author thanks both of the institutions for allowing her to use their data during her master thesis at Curtin University of Technology, Perth, W.A. Many thanks to Dr. Mehrooz Aspandiar and Dr. Thomas Cudahy for their great helps both in technical processing data and scientific comments.

References

Anand, R.R., Fraser, S.J., Jones, M.R., Shu, L., Munday, T.J., Phang, C., Robertson, I.M.D., Scoot, K.M., Vasconcelos, P., Wildman, J.E., and Wilford, J., 2002. *Geochemical explo-*

ration in regolith dominated terrain, North Queensland CRC LEME, Perth.

Anand R.R. and Paine, M.D., 2002. Regolith geology of the Yilgarn Craton, Western Australia; implications for exploration. *Australian Journal of Earth Sciences*, 49 (3), p.3-162.

Anand, R.R., Phang, C., Wilford, J., Wildman, J.E., Shu, L., Robertson, I.D.M., and Munday, T.J., 2002a. *Regolith-landscape characteristics, evolution and regional synthesis of the Mt. Isa Region*, 125, CRC-LEME, Perth.

Butt, C.R.M., 2005. Geochemical dispersion, process and exploration models. *In*: *Regolith Expression of Australian Ore Systems*. CRC LEME, p.81-106.

Blake, D.H., 1987. Geology of the Mount Isa Inlier and environs, Queensland and Nothern Territory. Bureau of Mineral Resources, *Geology and Geophysics, Australia, Bulletin*, 225 83pp.

Cudahy, T., Jones, M., Thomas, M., Laukamp, C., Caccetta, M., Hewson, R., Rodger, A., and Verrall, M., 2008. Next Generation Mineral Mapping: Queensland Airborne HyMap and Satellite ASTER Surveys 2006-2008, *CSIRO Exploration & Mining Report P2007/364.*

Clark, R.N., 1999. *Spectroscopy of Rocks and Minerals, and Principle of Spectroscopy*. U.S. Geological Survey, New York.

Drury, S., 2001. *Image Interpretation in Geology*. Blackwell Science.

Eriksson, K.A., Taylor, S.R., and Korsch, R.J., 1991. Geochemistry of 1.8-1.67 Ga mudstone and siltstone from the Mount Isa Inlier, Queensland, Australia: Provenance and tectonic implications. *Geochemica et Cosmochimia Acta*, 56, p.899-909.

Fujisada, H., 1994. Overview of ASTER instrument on EOS-AM1 platform. *Proceeding SPI 2268*, Infrared Spaceborn Remote Sensing II. DOI: 10.1117/12.185838

Geological Survey of Queensland, 2011. North-West Queensland mineral and energy province report and data package. Queensland Depatment of Employment, Economic Development and Innovation, 1V, 123pp, maps.

Gozzard, J.R., 2006. Image Processing of ASTER Multispectral Data. *In*: I.a. Resources (Ed). *Geological Survey of Western Australia*.

Gupta, R.P., 2003. *Remote Sensing Geology*. Springer.

Hewson, R.D., Cudahy, T.J., Drake-Brockman, J., Meyers, J., and Hashemi, A., 2006. Mapping geology associated with manganese mineralisation using spectral sensing techniques at Woodie Woodie, East Pilbara. *Exploration Geophysics*, 37, p.389-400. DOI: 10.1071/EG06389

Hewson, R.D., Cudahy, T.J., Mizuhiko, S., Ueda, K., and Mauger, A.J., 2005. Seamless geological map generation using ASTER in the Broken Hill-Curnamona province of Australia. *Remote Sensing of Environment*, 99 (1-2), p.159-172. DOI: 10.1016/j.rse.2005.04.025

Hunt, G.R., 1977. Spectral signature of particulate minerals in the visible and near infrared. *Geophysics*, 42 (3), p.501-513. DOI: 10.1190/1.1440721

Iwasaki A. and Fujisada, H., 2005. *ASTER Geometric Performance. IEEE Transaction on Geoscience and Remote Sensing*, 43(12). DOI: 10.1109/TGRS.2005.849055

Lewis, M., 2002. *Mapping Arid Vegetation Associations with HyMap Imagery*. IEEE Xplore. DOI: 10.1109/IGARSS.2002.1026781

Mars, J.C. and Rowan, L.C, 2006. Regional mapping of phyllic- and argillic-altered rocks in the Zagros magmatic arc, Iran, using Advanced Spaceborne Thermal Emission and Reflection Radiometer (ASTER) data and logical operator algorithms. *Geosphere*, 2, p.161-186.

Nahon, D. and Tardy, Y., 1992. The ferruginous laterites. *In*: Butt, C.R.M. & Zeegers, H. (eds), *Regolith Exploration Geochemistry in Tropical and Subtropical Terrains*. Elsevier Science Publishers.

Oliver, S. and van der Wielen, S., 2006. Mineral mapping with ASTER. *AusGeo News*, 82, 3pp.

Rowan, L.C. and Mars, J.C., 2003. Lithologic mapping in the Mountain Pass, California area using Advanced Spaceborne Thermal Emission and Reflection Radiometer (AS-

TER) data. *Remote Sensing of Environment*, 84 (3), p.350-366. DOI: 10.1016/S0034-4257(02)00127-X

Tapley, I.J. and Gozzard, J.R, 1992. Regolith-landform mapping in the Lawlers District. Report 1: Aerial photographic interpretation and Landsatt Thematic Mapper processing for mapping regolith-landforms, CSIRO Australia Division of Exploration and Mining, Perth. *Report 239R CSIRO/AMIRA Project P243*, 119pp. (Unpublished).

Taylor, G. and Eggleton, R.A., 2001. *Regolith Geology and Geomorphology*. John Willey, New York, 375pp. DOI: 10.1017/S0016756801216239

Van Ruitenbeek, F.J.A., Debba, P., van der Meer, F.D., Cudahy, T., van der Meijde, M., and Hale, M., 2006. Mapping white micas and their absorption wavelengths using hyperspectral band ratios. *Remote Sensing of Environment*, 102 (3-4), p.211-222. DOI: 10.1016/j.rse.2006.02.012